Analysis of Satellite Synthetic Aperture Radar Imagery of Alaska and Antarctic Radar Altimeter Data Acquired by the First European Remote Sensing Satellite (ERS-1)

Vera A. Voronina, Dennis R. Fatland, and *Craig S. Lingle,* Geophysical Institute, University of Alaska Fairbanks, Fairbanks, Alaska

ABSTRACT: *The synthetic aperture radar (SAR) and radar altimeter onboard the European Space Agency's First European Remote Sensing Satellite (ERS-1) have provided unprecedented coverage of the oceans, continents, glaciers, and ice sheets to latitude 82˚ N and S. A summary is given of software developed for: (i) optimal interpolation of U.S. Geological Survey digital elevation models (DEM's) using the geostatistical method of kriging, for use in terrain correction of full-resolution SAR imagery; (ii) kriging of irregularly-distributed SAR-image data onto the nodes of a regular grid, with velocity vectors measured on Bering Glacier, Alaska, during a recent surge employed as an example; and (iii) computation from radar altimeter data of a preliminary DEM of the West Antarctic ice sheet, which is considered potentially unstable because it is grounded well below sea level. The computations are carried out on the Cray Y-MP M98 and T3D Massively Parallel Processor of the Arctic Region Supercomputing Center.*

Introduction

The launch of the First European Remote Sensing Satellite (ERS-1) by the European Space Agency in July 1991 has resulted in extensive coverage of the oceans and continents by the onboard synthetic aperture radar (SAR)—which is a sideways-looking radar yielding images acquired in swaths—and of the oceans and polar ice sheets by the radar altimeter, which is a nadir-pointing instrument designed for measurement of surface elevations from timing of the range between the satellite and the surface. The microwave frequency (5.3 GHz, i.e., 0.057 m wavelength) of the C-band SAR onboard ERS-1 yields the advantage, over imagery relying on radiation within the visible range, of 'seeing through' clouds and darkness. The same advantage accrues to the 13.8 MHz (Ku band) radar altimeter. Among the problems that can be addressed with these instruments are the dynamic behavior and mass balance of glaciers and ice sheets—or, more specifically, their surface velocity, topography, and the time rate-of-change of their surface heights. These problems are of interest in conjunction with the close relationships among glaciers, ice sheets and climatic change, on time scales ranging from decades to thousands of years, and in conjunction with the problem of rising sea level [1]; [2]; [3].

SAR images are 'pictorial,' and often yield useful information without further modification. Terrain distortion is caused, however, by the side-looking nature of the radar, and this effect becomes severe in areas of high relief [4]. Also, sequential images of the same area may be acquired from spatially varying satellite positions, particularly if the satellite is not in an exact repeat orbit, causing terrain distortion to vary among different images of the same area. Terrain correction [5]; [6] can be employed for rectification, but digital elevation models (DEM's), which are a fundamental component of terrain correction, tend to be significantly coarser in resolution than full-resolution SAR images. A terrain corrected SAR image necessarily has resolution equal to the resolution of the underlying DEM. Software has thus been developed for estimation of the spatial structure in DEM's, and optimum interpolation of the elevations onto the nodes of a finer grid suitable for terrain correction of full resolution SAR imagery. Kriging is employed, which is a method for estimating the elevations at the grid nodes such that the error variance is minimized in a mean-square sense [7]. This software has also been adapted to krige other measured quantities, which may be irregularly distributed throughout non-uniform domains within SAR images, onto the nodes of a regular grid.

In addition, software has been developed to run on the Cray T3D, for computation of relatively high-resolution DEM's of the polar ice sheets via kriging of ice-sheet satellite radar altimeter data. These data have been acquired by ERS-1, and subse-

quently processed by the British Processing and Archiving Facility (U.K. PAF), then further processed into a form suitable for ice-sheet analysis at NASA Goddard Space Flight Center. Earlier ice-sheet radar altimeter data have been acquired by U.S. satellites; that is, by Seasat (1978) and Geosat (1985-1989), but these data [8] extend to 72˚ N and S. Computation is described of a preliminary DEM of the West Antarctic ice sheet (WAIS), which is almost entirely south of lat. 72˚ S, using ERS-1 altimetry. WAIS is thought to be potentially unstable because it is grounded well below sea level. (See, e.g.,[9]; also [10], and [11]. Surface topography is a key variable in the attempt to evaluate the dynamic behavior of WAIS, because of the key role of surface slopes in driving the flow of the ice sheet, and because disequilibrium is reflected in the time rate-of-change of the surface heights.

DEM Interpolation for Terrain Correction of Full-Resolution SAR Imagery

Terrain correction of SAR imagery offers the advantages of geocoding (rotation of the image to a standard orientation, such that north is 'up'), registration to a standard map projection (Universal Transverse Mercator [UTM]), and hence, referencing of the pixels to geographic coordinates (latitude-longitude, and UTM). Sequential SAR images of the same area are automatically coregistered to within about one pixel, due to being registered to the same underlying DEM. (In practice, a small additional displacement and/or rotation may be necessary for adequate coregistration.) It is thus possible to measure the absolute positions of features on the earth's surface, and changes in the positions of features that are moving.

Terrain correction consists, in essence, of using the DEM of the area corresponding to the area of a given SAR image, combined with knowledge of the position of the satellite at the time of the image acquisition, to compute—from the imaging geometry—a synthetic SAR image that includes terrain distortion. The real SAR image is then correlated with the synthetic image, by correlating discrete tiles of pixels that are distributed throughout the image area. The synthetic image is a function of the DEM, as is the real SAR image after correlation. The real image is then rectified (geometrically corrected) using the undistorted shape of the topography, as represented by the DEM. Detailed descriptions of this procedure are given by [4], [5], and [6]. The final terrain corrected product necessarily has pixels equal in size to the pixels of the underlying DEM. The DEM of Alaska [12] is defined on a grid which is, at the latitude of southern Alaska, approximately 90 m square.

Prior to the July 1991 launch of ERS-1, the terrain correction software developed by [6] was implemented on the Sun 4/280-based interactive image analysis system of the Alaska SAR Facility (ASF) by R.M. Guritz, of ASF, and was found suitable for terrain correction of low-resolution SAR images, which have 100 m pixels and a resolution of 240 m. However, full-resolution SAR images—which have 12.5 m pixels and a resolution of 30 m—are necessary for many applications. Use of USGS 90 m DEM's for terrain correction of full-resolution SAR imagery results in unacceptable loss of resolution.

Software was therefore developed to quantify the spatial structure in the DEM elevation data throughout regions of glaciological interest. Variograms are employed (see, e.g.,[7]), which are analogous to autocorrelation functions in time series analysis. The elevations of the DEM are then estimated on a 30 m grid by ordinary kriging, using the 16 nearest elevations of the surrounding grid. Briefly, a linear system of 17 equations is solved for the optimum weights (which minimize the error variance) and a LaGrange multiplier at each node. The unknown elevation is then estimated as an optimally weighted, unbiased linear combination of the surrounding known elevations. Computational efficiency is attained by exploiting the symmetry of the square grid, and by utilizing multiple processors (8) on the T3D combined with direct-access I/O.

The resulting 'enhanced' 30 m DEM's do not, of course, contain elevation information beyond what is contained in the original 90 m DEM's, which have an estimated vertical accuracy (feature to mean sea level) of + 30 m, linear error at 90% probability, and a horizontal accuracy of 130 m, circular error at 90% probability [12]. The additional vertical error introduced by kriging was evaluated by making use of a 672 km^2 subarea of a relatively high-resolution DEM of the Juneau Icefield, in the Northern Coast Mountains of Southeast Alaska, which is defined on a 60 m grid (Figure 1a). Alternate nodes of the 60 m grid were discarded. The missing elevations were then kriged back in, using the remaining elevations spaced at 120 m, and compared to the original (discarded) elevations. The mean-squared difference was found to be 2.34 m^2 throughout the area, suggesting that an average additional uncertainty of about ± 1.5 m, relative to the original DEM, is introduced by kriging. This is small compared to the ± 30 m mean accuracy of a 90 m DEM. Figure 1b shows a contour map of the area of Figure 1a, indicating a transect (Tr. 1) along which the differences between the kriged elevations (solid line) and the original elevations (datum) are shown in Figure 1c. The dashed line shows the difference between the original (discarded) elevations and the elevations along the same transect, estimated using the more conventional but less accurate method of bilinear interpolation. Other transects yielded difference plots roughly similar to Figure 1c.

DEM's kriged to a resolution of 30 m have been found to yield substantially improved results when terrain correcting full-resolution SAR imagery of the heavily glacierized terrain of southern Alaska, using the terrain-correction software developed, originally, by [6]. More recently, this software has been adapted and optimized to run on the T3D [13]. The resulting great increase in computational speed has made it feasible to terrain correct entire full-resolution SAR images. (Previously only relatively small subscenes, or low-resolution SAR images, could be terrain corrected.) The resulting images, terrain corrected to a resolution of 30 m, have significantly improved map-plane resolution due to retention of an increased number of

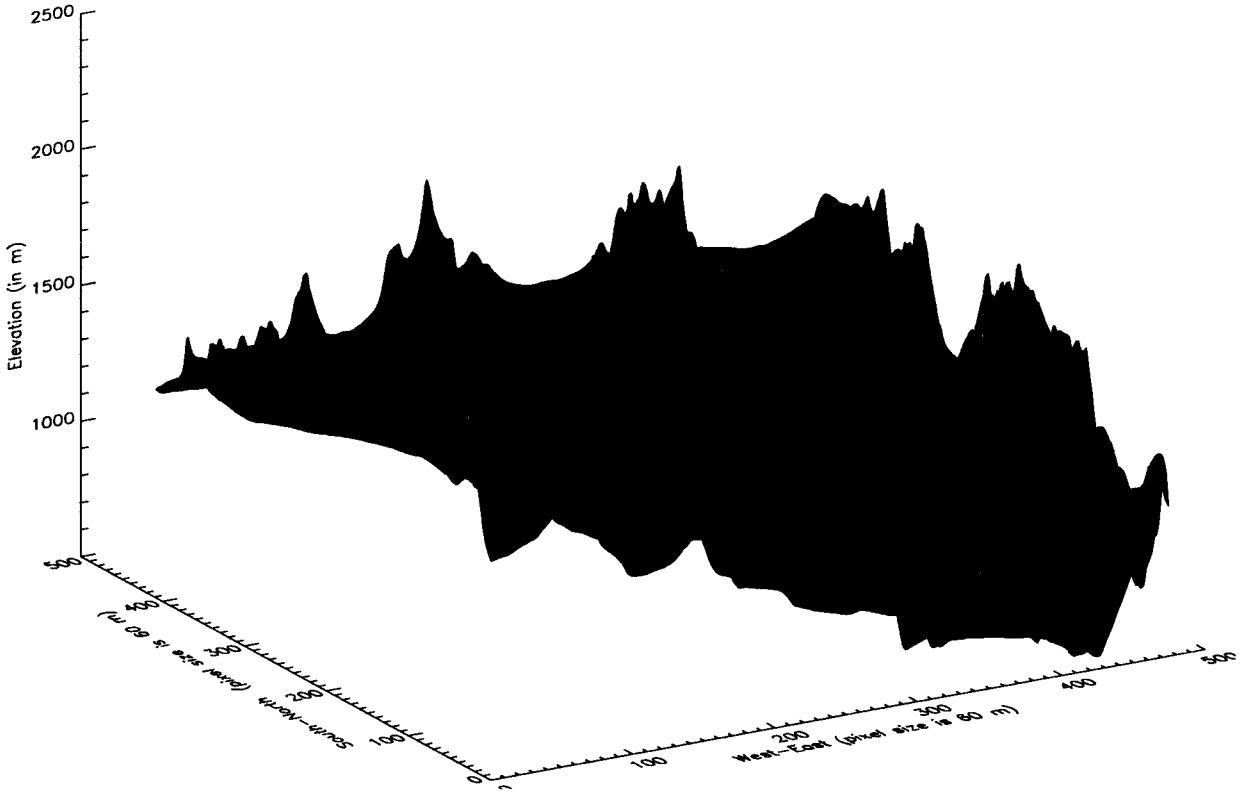

Figure 1a: Surface map of the 60 m USGS digital elevation model (DEM) of a 24 km x 28 km area of the Juneau Icefield, Alaska. The precipitous rock peaks are nunataks (islands) projecting through the connected glaciers of the Northern Coast Mountains. The vertical scale is elevation above sea level, in meters. The horizontal scales are distance, in multiples of 60 m (the pixel size).

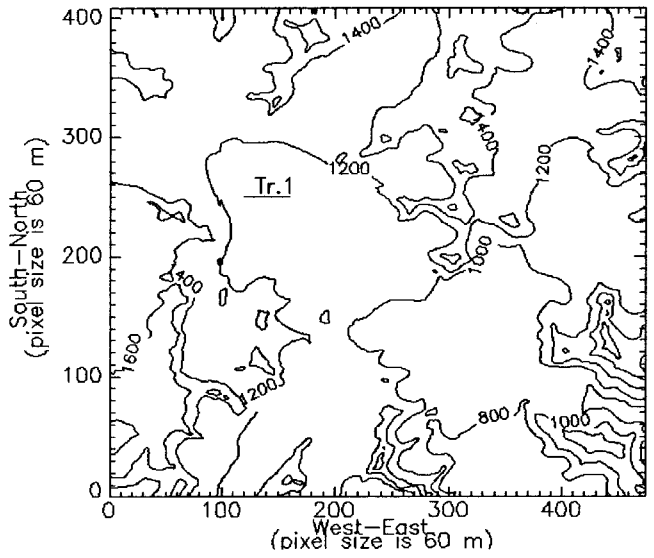

Figure 1b: Contour map of the area shown in Figure 1a. Elevation contours and horizontal scales are as in Figure 1a. 'Tr. 1' is the transect shown in Figure 1c.

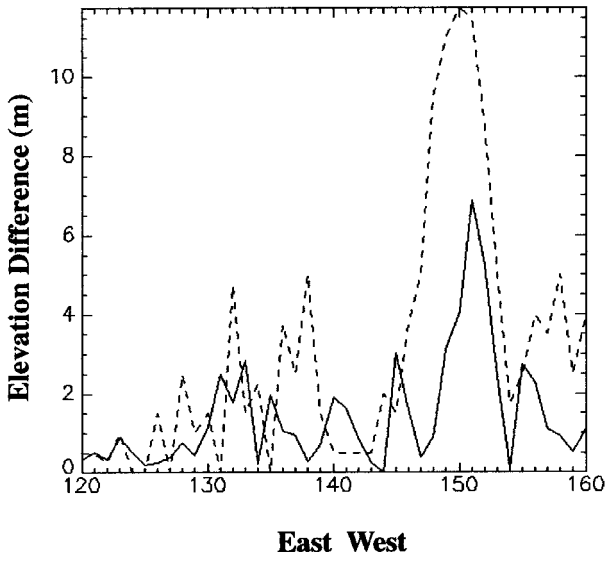

Figure 1c: Absolute difference between grid point elevations estimated using the optimal interpolation method of kriging (solid line), and bilinear interpolation (dashed line), and the original DEM elevations at the same grid points, which were 'discarded' (datum), for Transect 1 in Figure 1b.

'in-between' pixels when the original full-resolution images are registered to the DEM. This improved map-plane resolution occurs in spite of the increased vertical error caused by kriging of the DEM onto a finer grid.

SAR-Derived Velocity on Lower Bering Glacier During Surge

During spring 1993, a surge of the Bering Glacier began in the Chugach Mountains of Southcentral Alaska [14]; [15]; [16]. A glacier surge is a dramatic acceleration of flow lasting one to several years, resulting in an advance of the terminus of the order of 1 to 10 km, after a period of quiescence and retreat lasting of the order of 20 to 50 years. Glacier surges are cyclic (see, e.g., [17]). A description of the Holocene (past 8,000 year) history of Bering Glacier is given by [18]. The surge provided an ideal opportunity for observation and measurement using spaceborne SAR imagery, since Bering Glacier—which has a total area, including tributaries, of 5,200 km^2 [14]—is the largest glacier in North America, and in the world outside Antarctica and Greenland. Its length, from ice divide in the St. Elias Mountains to calving terminus in Vitus Lake, on the Gulf of Alaska coast, is 185 km. The main trunk has an average width of about 10-12 km.

Velocities were measured on the lower glacier by coregistering subscenes from two images acquired 9 August and 13 September 1993, during the 35-day exact repeat orbit cycle of ERS-1, which is the time interval during which the propagating surge front reached the calving terminus of the glacier. The images were coregistered visually to within about one pixel, using areas of fixed topography (not moving ice). Complex, full-resolution, slant-range images that were not terrain corrected were used, in order to maximize resolution. These images have pixel dimensions of 7.9 m (range) by 3.9 m (azimuth). Power-domain averages over 5 pixels in the azimuth direction were taken, increasing that pixel dimension to 19.5 m. The 7.9 m slant-range pixels correspond to about 20 m in ground range, so the averaged pixels had aspect ratios close to 1.

The displacements of features on the moving glacier, which could be recognized in both subscenes, were then measured directly. Care was taken to avoid features, such as some crevasses, which were deforming so rapidly that they changed visibly during the 35-day interval between the images. The measured displacements, expressed as velocity (meters per day), are shown in Figure 2a. The combination of errors from SAR imaging geometry, image misregistration, and ambiguities in feature identification result in errors of less than 10% (approximately) in the initial velocity measurements, derived from the relatively large ice displacements associated with the surge.

The measured velocity vectors (Figure 2a) were then kriged onto the nodes of a 1 km square grid. Spatial structure was estimated by computing two variograms for the two horizontal components of the velocity vectors, which were then kriged independently. The results are shown in Figure 2b. The error of each of the kriged velocity vectors has two components: one due to the measurement errors described above, and a second, generally larger component that is due to the spatial distance between the measured vectors and the grid nodes. The first component is propagated through the kriging equations, using standard methods. The second component is estimated from the variance at the kriged nodes. Only the vectors having combined error less than 30% of the total velocity are retained in Figure 2b, which shows that many of the velocity vectors are in the 10-20 m/day range. The maximum ice velocity shown in Figure 2b is 59 m/day. This can be compared to the quiescent period between surges, when the surface velocities were of the order of 1 m/day (R. Krimmel, pers. comm.) or less [19]. Shortly after the image of 13 September 1993 was acquired, Vitus Lake filled with icebergs as the terminus advanced rapidly.

Figures 2a and 2b illustrate the rapid ice displacements and high deformation rates that can occur on a massive scale, given destabilization and transformation of the basal hydraulic system such that the glacier is partially decoupled from its bed. For a detailed description of the surge process, based on comprehensive measurements of a smaller surge-type glacier, see [20].

The problem of kriging velocity vectors on lower Bering Glacier is rather more specialized, requires substantially more judgement, and is less computationally intensive than the problem of kriging DEM's, which can be done automatically. The software employed to obtain the results shown in Figure 2b was developed to run on the ARSC Cray Y-MP M98. It would be computationally advantageous to adapt this software to run on the T3D, particularly for larger sets of irregularly distributed data, but this has not yet been done.

A Preliminary DEM of the West Antarctic Ice Sheet

The potential instability of the West Antarctic Ice Sheet (WAIS), which was pointed out by [21], has been summarized more recently by [9]. Briefly, WAIS can be considered a large-scale analog of Columbia Glacier, which descends from the Chugach Mountains of Southcentral Alaska and is grounded in a deep fjord, in Prince William Sound. The stability of Columbia Glacier was maintained, since the first recorded observation in 1794, as a result of the terminus being grounded on a shallow moraine sill at the seaward end of Columbia Fjord. (Characteristically, glacier-carved fjords are relatively shallow [order 10-100 m] at their seaward ends, and attain greatest depth [order 400-600 m] near their inland ends, due to more vigorous basal erosion beneath the thicker ice farther up the fjord.) Irreversible retreat began when the terminus of Columbia Glacier retreated into deeper water upglacier from the terminus, which resulted in dramatic acceleration of flow, accompanied by an even greater acceleration of iceberg calving [22]. Disintegration has continued through the present, and is expected to continue until the terminus retreats to the inland end of Columbia Fjord, where the glacier bed (i.e., fjord bottom) rises above sea level. WAIS, which is grounded below sea level on ocean floor up to 2,000 m deep [23], is considered subject to an analogous form of

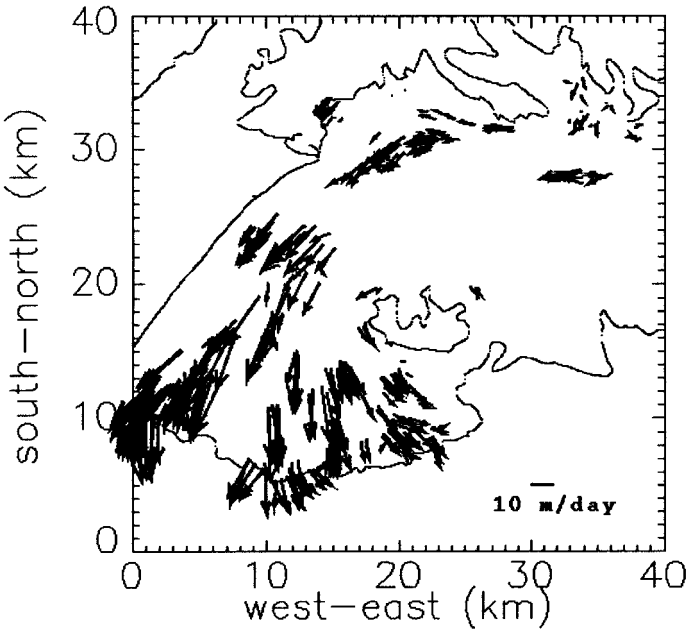

Figure 2a: Velocity vectors measured on Bering Glacier, Alaska, during its (1993-1995) surge. The displacements of recognizable features were measured in two coregistered ERS-1 SAR images separated by 35 days. The higher concentration of vectors on the lower glacier corresponds to a higher density of recognizable features on the rougher, chaotically—crevassed surface.

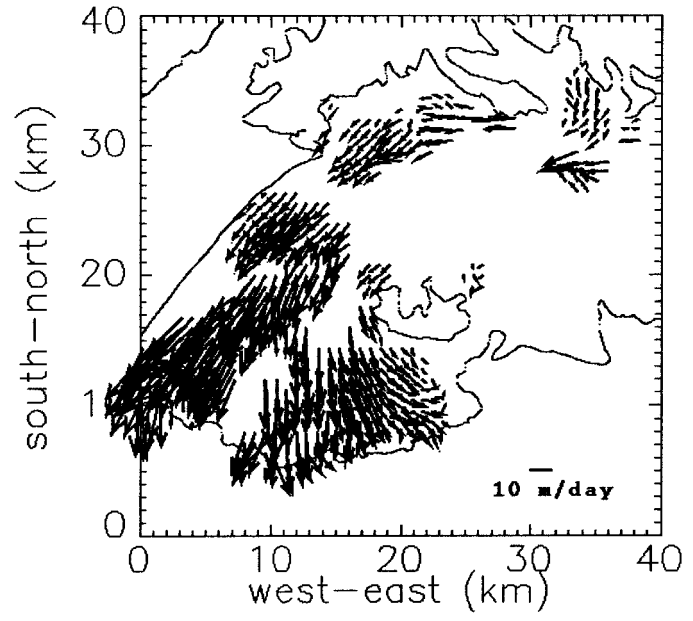

Figure 2b: Velocity vectors on lower Bering Glacier, kriged onto a 1 km square grid using the data shown in Figure 2a. The error of each vector was computed; vectors with errors greater than 30% of the total magnitude were eliminated. The maximum velocity shown here is 59 m/day. The gridded velocities are suitable for computation of the principal strain rate components (not shown) which reflect the ice deformation.

marine instability. Complete disintegration would raise global mean sea level by about 6 m. It is thought that this process, if it occurs, could proceed to completion on a time scale of about 500 to 1,000 years [2].

Ice sheets flow in response to the driving stress, which is proportional to the product of the ice thickness and the surface slope, acting in conjunction with hydraulic processes which enable basal sliding, in areas where water is present at the bed [17]. An accurate DEM of the surface topography is thus a fundamental component of ice-sheet models. ERS-1 has, for the first time, extended satellite altimeter coverage of the ice sheets to a sufficiently high southern latitude to include about two-thirds of the West Antarctic ice sheet.

A preliminary DEM of WAIS has been kriged on a relatively high-resolution 3 km grid (Figures 3a, 3b), using ERS-1 Antarctic altimeter data retracked by H.J. Zwally's ice-sheet altimetry group at NASA Goddard Space Flight Center (GSFC). The data set employed for this computation did not include slope corrections, and close examination of the results suggests that orbit problems may be present in the data (J. Dimarzio, pers. comm.). More recently, updated ERS-1 Antarctic altimeter data have been received from GSFC, including improved precision orbits, slope corrections, and tropospheric and ionospheric corrections, in addition to retracking. The results shown in Figures 3a, 3b should thus be interpreted only as an initial 'rough cut.'

The software used for kriging of the DEM shown in Figures 3a, 3b was developed to run on the Cray T3D. An earth-centered spherical coordinate system was employed, since the area of WAIS is too large for conversion to a single universal transverse mercator (UTM) projection. (A UTM projection, with orthogonal coordinate axes and distances in meters, would normally be the projection of choice for areas of more limited size. See, e.g., [24]). WAIS was divided into 21 subareas, each the same in terms of latitude-longitude coverage. (The latitude range spanning WAIS was divided into 3, and the longitude range into 7.) The spatial structure in the data was then quantified by computing a global variogram for each subarea. The horizonatl lags between the elevation data of the variograms were computed in terms of spherical arc length on the earth's surface. The variograms were represented, for use in the kriging equations, by least-squares best-fit Gaussian models. The closest 24 elevation data, selected in a quadrant search (6 points per quadrant), were used to krige each node. The data from only one 35-day orbit cycle of ERS-1 were used, in order to limit the quantity of data employed in the computation. Data from more orbit cycles would increase the coverage, in the sense that data gaps would tend to be progressively filled in, but the pattern of coverage—i.e., the orbit geometry—would remain the same, as long as data from the 35-day orbit cycle were utilized.

Four T3D processors were employed for this preliminary computation. Within each subarea the computation was carried out along parallels of latitude, with processors 1-4 kriging nodes n, n +1, ..., n +4. More processors will be used in the future, to

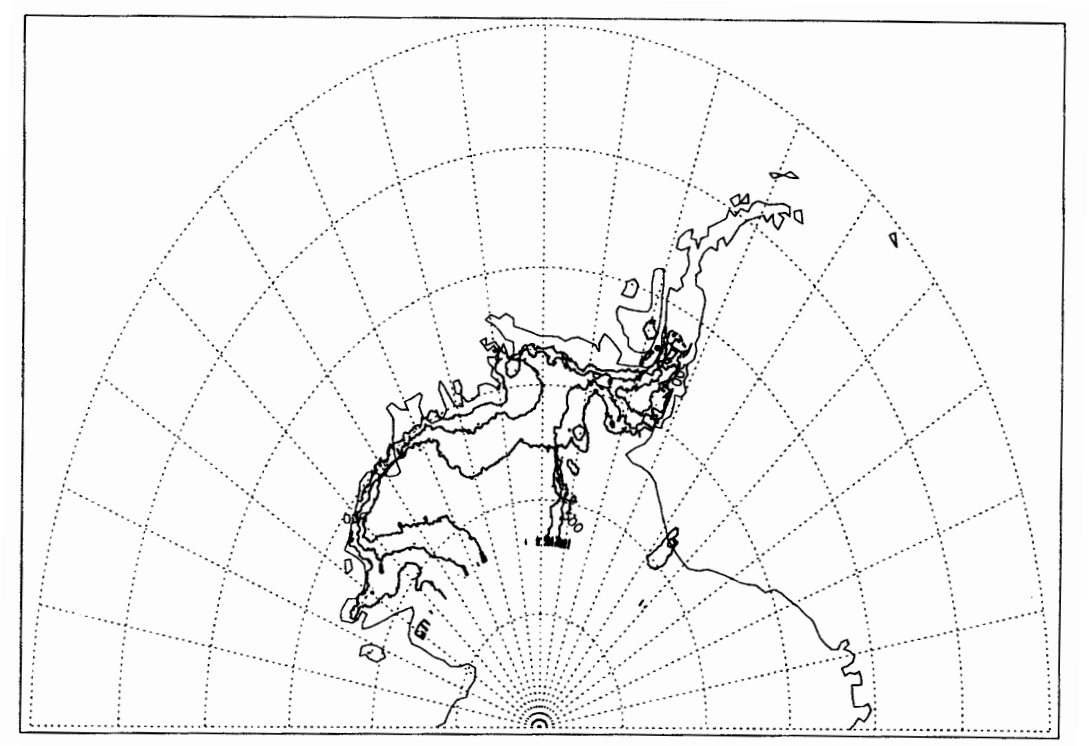

Figure 3a: Preliminary digital elevation model (DEM) of the West Antarctic ice sheet, computed from ERS-1 altimetry. The South Pole is at bottom-center. The Antarctic Peninsula (top, right of center) points in the direction of South America. The contour interval is 500 m. The highest elevations shown are 2,000 m. The contours are truncated at 82° S, which is the southernmost extent of orbital coverage.

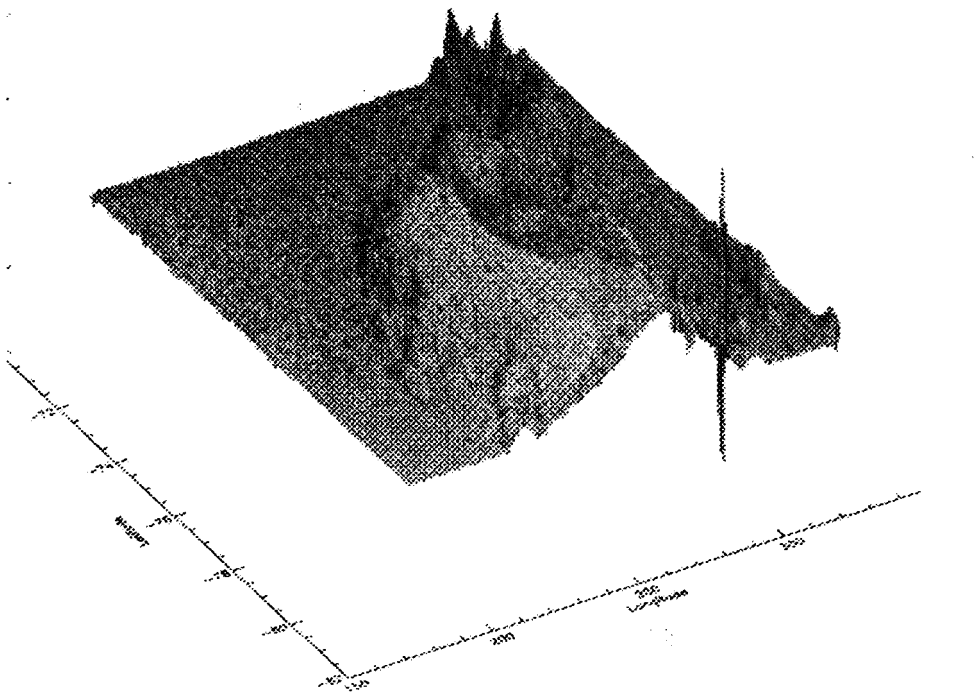

Figure 3b: Gray-scale surface map of the preliminary DEM of the West Antarctic ice sheet shown in Figure 3a. The spikey surface in center-distance is the mountainous Antarctic Peninsula. The low-elevation surface in center-foreground is the Ross Ice Shelf, which is approximately south of New Zealand. The prominent ridge in the center is the West Antarctic divide.

handle the greatly increased volumes of data that are now available.

The results (Figures 3a, 3b) show that it is clearly feasible, in a computational sense, to compute large-scale ice sheet DEM's on a grid as fine as 3 km, using the T3D. The surface elevations are somewhat noisy, however, which suggests that low-pass filtering of the along-track data should be carried out prior to kriging. A description of a suitable filtering method is given by [25].

Summary

Geostatistical methods have been employed for: (i) estimation of spatial structure and optimal interpolation (kriging) of USGS digital elevation models onto a finer grid suitable for terrain correction of full-resolution spaceborne synthetic aperture radar (SAR) imagery; (ii) kriging of the irregularly distributed velocity vectors—measured with SAR imagery on a large Alaskan glacier during a recent surge—onto a regular grid, suitable for computation of the principal strain rate components that measure ice deformation; and (iii) computation of a relatively high-resolution digital elevation model—from satellite radar altimeter data—of the potentially unstable West Antarctic ice sheet. The software for this work has been developed to run on the Cray Y-MP M98 and T3D systems of the Arctic Region Supercomputing Center (ARSC). The results show that the ARSC Cray system is well suited for analysis of the massive data sets generated by earth observation satellites such as ERS-1.

Acknowledgments

This work has been supported by Cray Research, Inc., 1994 and 1995 University Research and Development Grant Program awards to C. Lingle and V. Voronina, by National Science Foundation grant OPP-9319873 and NASA grant NAGW-4371 to C. Lingle, and by NASA grant NAGW-2827 to C. Lingle and W. Harrison. We thank the Arctic Region Supercomputing Center of the University of Alaska Fairbanks for providing grants of computational resources, and J. Zwally, of Goddard Space Flight Center, and A. Brenner and J. Dimarzio, of Hughes STX Corp., for furnishing retracked ERS-1 altimeter data from the Antarctic ice sheet.

References

[1] Folland, C.K., T.R. Karl, and K.YA. Vinnikov. 1990. Observed climate variations and change. In: *Climate Change: The IPCC Scientific Assessment*, pp. 195-238, Cambridge University Press, New York.

[2] National Research Council. 1985. *Glaciers, Ice Sheets and Sea Level: Effects of a CO^2-Induced Climatic Change*. National Academy Press, Washington, D.C., U.S.A., 330 pp.

[3] Warrick, R., and J. Oerlemans. 1990. Sea level rise. In: *Climate Change: The IPCC Scientific Assessment*, pp. 258-281. Cambridge University Press, New York.

[4] Curlander, J.C., and R.N. McDonough. 1991. *Synthetic Aperture Radar: Systems and Signal Processing*. John Wiley and Sons, 647 pp.

[5] Kwok, R., J.C. Curlander, and S.S. Pang. 1987. Rectification of terrain induced distortions in radar imagery. *Photogrammetric Engineering and Remote Sensing*, 53(5), 507-513.

[6] Wivell, C.E., D.R. Steinwand, G.G. Kelly, and D.J. Meyer. 1992. Evaluation of terrain models for the geocoding and terrain correction of synthetic aperture radar (SAR) images. *IEEE Trans. Geosci. and Remote Sensing*, 30(6), 1137-1143.

[7] Isaaks, E.H., and Srivastava, R.M. 1989. *Applied Geostatistics*. Oxford University Press, New York.

[8] Zwally, H.J., and R.A. Bindschadler. 1995. Ice Altimetry System. CD-ROM containing ice altimetry data for Greenland and Antarctica from Seasat and Geosat GM missions. Available from National Snow and Ice Data Center, CIRES, University of Colorado, Boulder, CO 80309-0449, U.S.A.

[9] Alley, R.B., and I.M. Whillans. 1991. Changes in the West Antarctic ice sheet. *Science*, 254 (5034), 959-963.

[10] *Journal of Geophysical Research*. 1987. Fast glacier flow issue, 92(B9), 8835-9134.

[11] *Journal of Glaciology*. 1993. Siple Coast issue, 39(133), 437-572.

[12] U.S. Geological Survey. 1990. *Digital Elevation Models: Data Users Guide 5*, National Mapping Program Technical Instructions, 51 pp.

[13] Logan, T.A. 1994. Terrain correction of synthetic aperture radar imagery using a Cray T3D scalable parallel processor. MS thesis, University of Alaska Fairbanks, 79 pp.

[14] Molnia, B. 1993. Major surge of the Bering Glacier. *EOS* 74(29), 321-322.

[15] Lingle, C.S., A. Post, U.C. Herzfeld, B.F. Molnia, R.M. Krimmel, and J.J. Roush. 1993. Bering glacier surge and iceberg-calving mechanism at Vitus Lake, Alaska, U.S.A. (correspondence). *J. Glaciol*., 39(133), 722-727.

[16] Roush, J.J., C.S. Lingle, and R.M. Guritz. The 1993-'94 surge of Bering Glacier, Alaska, observed with ERS-1 synthetic aperture radar imagery. Submitted to *Journal of Glaciology*.

[17] Paterson, W.S.B. 1994. *The Physics of Glaciers*. Third edition, Pergamon, 480 pp.

[18] Molnia, B.F., and A. Post. 1995. Holocene history of Bering Glacier, Alaska: A prelude to the 1993-1994 surge. *Phys. Geog*., 16(2), 87-117.

[19] Post, A. 1972. Periodic surge origin of folded medial moraines on Bering piedmont glacier, Alaska. *J. Glaciol*., 11(62), 219-226.

[20] Kamb, B., C.F. Raymond, W.D. Harrison, H. Engelhardt, K.A. Echelmeyer, N. Humphrey, M.M. Brugman, and T. Pfeffer. 1985. Glacier surge mechanism: 1982-1983 surge of Variegated Glacier, Alaska. *Science*, 227, 469-479.

[21] Hughes, T. 1973. Is the West Antarctic ice sheet disintegrating? *J. Geophys. Res*., 78(33), 7884-7910.

[22] Meier, M.F., L.A. Rasmussen, and D.S. Miller. 1985. Columbia Glacier in 1984: Disintegration underway. U.S. Geological Survey Open-File Report 85-81.

[23] Drewry, D.J. (ed.) 1983. *Antarctica: Glaciological and Geophysical folio*. Scott Polar Research Institute, University of Cambridge, Cambridge, U.K.

[24] Herzfeld, U.C., C.S. Lingle, and L.-h. Lee. 1994. Recent advance of the grounding line of Lambert Glacier, Antarctica, deduced from satellite-radar altimetry. *Ann. of Glaciol*., 20, 43-47.

[25] Lingle, C.S., L.-h. Lee, H. J. Zwally, and T.C. Seiss. 1994. Recent elevation increase on Lambert Glacier, Antarctica, from orbit cross-over analysis of satellite-radar altimetry. *Ann. Glaciol*., 20, 26-32.,